structure was solved by a combination of direct methods and Fourier techniques. All hydrogen atoms were clearly visible in a difference Fourier synthesis phased on the non-hydrogen parameters. All hydrogen atoms were refined isotropically and non-hydrogen atoms anisotropically in the final cycles.

A final difference Fourier map was featureless, with the two largest peaks of 1.3 e/Å^3 each lying within 0.5 Å of the two W atoms. All other peaks were less than 0.7 e/Å^3.

Computational Procedures. Molecular orbital calculations were performed on a VAX computer system using the semiempirical methods of Fenske–Hall[21] and extended Hückel.[30] For the Fenske–Hall calculations, atomic wave functions were supplied by Professor M. B. Hall from Texas A&M University. Contracted double-ζ representations were used for the W 5d, O 2p, and C 2p atomic orbitals. In the basis function for tungsten, the 6s and 6p exponents were fixed at 2.40. All Fenske–Hall calculations were converted with a self-consistent field iterative technique by using a convergence criteria of 0.0010 as the largest deviation between atomic orbital populations for successive cycles.

The calculations were carried out on the hypothetical molecule $W_2(OH)_6(\eta^2\text{-}C_2H_4)_2$. The OH and CH bond distances were set at 0.96 and 1.08 Å, respectively, and other distances were obtained from the crystal structure or adapted to C_2 symmetry. The W–O terminal distances were set at 1.888 Å and W–O bridging distances in the asymmetric structure were 2.309 and 1.993 Å. Symmetric bridges had W–O distances of 2.15 Å. The W–C bond distance was averaged to 1.45 Å. The hydroxide ligands and the centroid of the ethylene C–C bonds were idealized so as to lie in two mutually perpendicular planes. The C–C bond axis of the ethylene ligand was oriented perpendicular to the plane containing the tungsten atom, the terminal OH ligand, and the C–C midpoint. In the Fenske–Hall calculations, the terminal OH bonds were constrained to be linear and the bridging hydroxide bonds planar, and the OH group was pointing such that it was perpendicular to the W–W bond axis.

The structural parameters for the intermediate in the fluxional process came from a combination of the crystal structure of $W_2(OCH_2\text{-}t\text{-}Bu)_6(\eta^2\text{-}C_2H_4)_2$ and $W_2(CH_2Ph)_2(O\text{-}i\text{-}Pr)_4(\eta^2\text{-}C_2Me_2)_2$.[32a] The distances were taken from $W_2(OCH_2\text{-}t\text{-}Bu)_6(\eta^2\text{-}C_2H_4)_2$, and the angles were taken from $W_2(CH_2Ph)_2(O\text{-}i\text{-}Pr)_4(\eta^2\text{-}C_2Me_2)_2$, in that the geometry about each W atom was taken to be square pyramidal with the alkoxide ligands occupying the base of the pyramid. In the latter molecule the bridges are asymmetric, but here they were made to be symmetric. The molecule was idealized to C_{2v} symmetry. With the structural parameters chosen in this way, the structure has not been optimized.

The extended Hückel calculations that examined the trans influence of the terminal ligands used W–O–C angles of the crystal structure for the W–O–H angles, although the addition of these angles was not found to change the results significantly.

Acknowledgment. We thank the Department of Energy, Office of Energy Research, Division of Chemical Sciences, for support. S.T.C. thanks the American Association of University Women Educational Foundation for an American Dissertation Year Fellowship. The Laboratoire de Chimie Théorique is associated with the CNRS (URA 506) and member of ICMO and IPCM. We also thank the NSF and CNRS under the US–France Cooperative Science Program.

Supplementary Material Available: Tables of anisotropic thermal parameters, complete listings of bond distances and bond angles, VERSORT drawings, and an Arrhenius plot of the kinetic data (13 pages); listing of F_o and F_c values (12 pages). Ordering information is given on any current masthead page.

Magnetic Properties of High-Nuclearity Spin Clusters. Fourteen- and Fifteen-Oxovanadium(IV) Clusters

Anne-Laure Barra,[†,§] Dante Gatteschi,*[,†] Luca Pardi,[†] Achim Müller,*[,‡] and Joachim Döring[‡]

Contribution from the Department of Chemistry, University of Florence, Florence, Italy, and Fakultät für Chemie, Universität Bielefeld, Bielefeld, Germany. *Received March 6, 1992*

Abstract: The magnetic properties of $K_6[V_{15}As_6O_{42}(H_2O)]\cdot 8H_2O$ (V_{15}) and $(NH_4)_6[V_{14}As_8O_{42}(SO_3)]$ (V_{14}) which comprise fifteen- and fourteen-vanadium(IV) ions, respectively, have been investigated. The analysis of the magnetic susceptibility and of the EPR spectra showed the presence of several different exchange pathways, which were identified also with the help of extended Hückel calculations. The analysis of the data was performed using both a perturbation and a rigorous approach within the spin hamiltonian formalism, allowing for the first time a deep insight into the energy levels of high nuclearity spin clusters.

Introduction

Molecular materials are actively investigated because with the approaches of molecular chemistry it is possible to fine tune their properties and obtain materials that can perform many of the functions traditionally associated with two- and three-dimensional network solids.[1-6]

One of the fields where exciting developments are reported almost every month is that of molecular based magnetic materials.[2,7-13] In this area several attempts have been made to design and synthesize "organic ferromagnets" or molecular materials exhibiting spontaneous magnetization below a critical temperature.

Another area of turmoil is that of high nuclearity spin clusters, HNSC, i.e. molecular materials containing large, but finite, numbers of spins which are coupled to each other.[14-18] For instance, manganese clusters containing up to 12 ions[19,20] and iron clusters containing up to 17 ions[21] recently have been reported in connection with the investigation of molecular models of bio-

[†] University of Florence.
[§] On leave of absence from SNCI, CNRS, Grenoble.
[‡] University of Bielefeld.

(1) Miller, J. S. *Adv. Mater* **1990**, *2*, 98.
(2) *Magnetic Molecular Materials*; Gatteschi, D.; Kahn, O.; Miller, J. S.; Palacio, F., Eds.; Kluwer: Dordrecht, 1991.
(3) *Molecular Electronic Devices*; Carter, F. L., Ed.; Marcel Dekker: New York, 1982. *Molecular Electronic Devices II*; Carter, F. L., Ed., Marcel Dekker: New York, 1987.
(4) *Materials for Nonlinear Optics, Chemical Perspectives*; Mardez, S. R.; Sohn, J. E.; Stucky, G. D.; ACS Symposium Series No. 455; American Chemical Society: Washington, DC, 1991.
(5) Kini, A. M.; Geiser, U.; Wang, H. H.; Carlson, K. D.; Williams, J. M.; Kwok, W. K.; Vandervoort, K. G.; Thompson, J. E.; Stupka, D. L.; Jung, D.; Whangbo, M. H. *Inorg. Chem.* **1990**, *29*, 2555.
(6) Manriquez, J. M.; Yee, G. T.; Scott McLean, R.; Epstein, A. J.; Miller, J. S. *Science* **1991**, *252*, 1415.
(7) Broderick, W. E.; Thompson, J. A.; Day, E. P.; Hoffman, M. *Science* **1990**, *249*, 910.
(8) Caneschi, A.; Gatteschi, D.; Rey, P. *Prog. Inorg. Chem.* **1991**, 39.
(9) Allamand, P. M.; Khemani, K. C.; Koch, A.; Wudl, F.; Holczer, K.; Donovan, S.; Gruener, G.; Thompson, J. D. *Science* **1991**, *253*, 301.

0002-7863/92/1514-8509$03.00/0

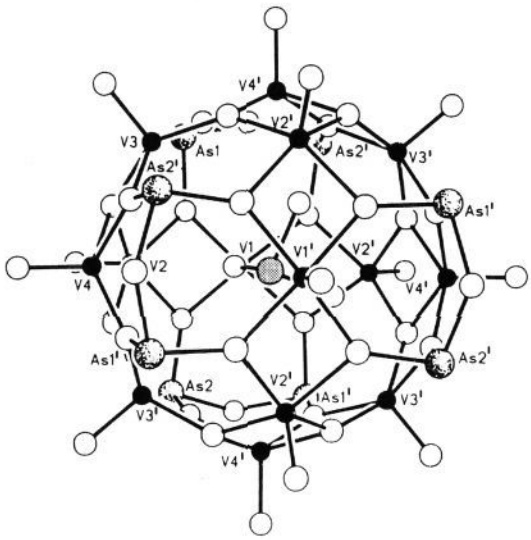

Figure 1. Structure of V_{14}.

logically relevant materials. The magnetic properties of these compounds have shown the presence of some unusual magnetic properties in general associated with mesoscopic scale magnetic particles.

An exciting class of HNSC based on polyvanadates recently has been reported.[18,22-31] These clusters comprise up to 34 vanadium ions, with formal oxidation states ranging from four to five. These materials have been suggested to be relevant to catalysis, to model the properties of bulk oxides, such as VO_2 and V_2O_5, and to investigate magnetic particles formed by large assemblies of spins.

In a preliminary report[32] we showed that $K_6[V_{15}As_6O_{42}(H_2O)]\cdot 8H_2O$, V_{15}, comprising fifteen vanadium(IV) ions, has a unique magnetic multilayer structure. We report here in more detail its magnetic properties, together with those of $(NH_4)_6[V_{14}As_8O_{42}(SO_3)]$, V_{14}, which comprises fourteen vanadium(IV) ions.[28] In particular we want to show how it is possible to obtain a detailed understanding of the structural basis of the magnetic properties of these HNSC, using a perturbation and a full matrix approach, within the spin hamiltonian formalism. These results allow us to establish structural–magnetic correlations for vanadium(IV) pairs, taking advantage of simple extended Hückel calculations.

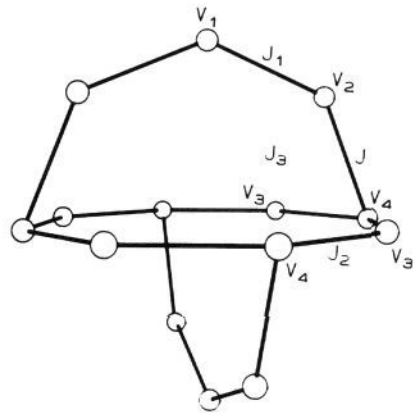

Figure 2. Outline of the vanadium ions of V_{14} and coupling constants.

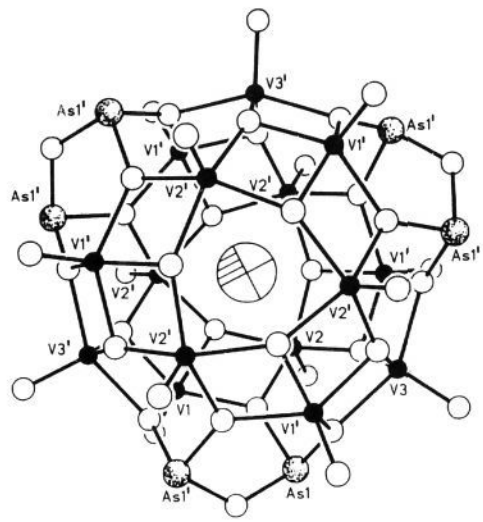

Figure 3. Structure of V_{15}.

Table I. Exchange Pathways and Coupling Constants in V_{14} and V_{15}

atom 1	atom 2	bridge 1	bridge 2	dist, Å	coupl const, cm^{-1}
		V_{14}			
V_1	V_2	AsO	AsO	3.10	J_1
V_2	V_3	O		3.60	J_3
V_2	V_4	O	O	2.81	J
V_3	V_4	O	AsO	3.01	J_2
		V_{15}			
V_1	V_2	O	O	2.87	J
V_1	V_2'	O	AsO	3.05	J'
V_1	V_3	O	AsO	3.02	J_1
V_2	V_2'	O		3.68	J''
V_2	V_3'	O		3.73	J_2

Experimental Section

Both V_{14} and V_{15} were prepared as previously described.[23,28] Single crystal EPR spectra were recorded with a conventional VARIAN E9 spectrometer operating at X-band frequency, equipped with a continuous flow ESR9 Oxford Instruments apparatus. The magnetic susceptibility was measured with a SQUID magnetometer built by Metronique Ingenierie.

(10) Pei, Y.; Kahn, O.; Nakatami, K.; Codjovi, E.; Mathioniere, C.; Sletten, J. *J. Am. Chem. Soc.* **1991**, *113*, 6558.
(11) Kaisaki, D. A.; Chang, W.; Dougherty, D. A. *J. Am. Chem. Soc.* **1991** *113*, 2764.
(12) Inone, K.; Koga, N.; Iwamura, H. *J. Am. Chem. Soc.* **1991**, *113*, 9803.
(13) Fujita, I.; Teki, Y.; Takui, T.; Kinoshita, T.; Itoh, K.; Miko, F.; Sawaki, Y.; Izuoka, A.; Sugawara, T.; Iwamura, H. *J. Am. Chem. Soc.* **1990**, *112*, 4074.
(14) Gorun, S. M.; Papaefthymion, G. C.; Frankel, R. B.; Lippard, S. J. *J. Am. Chem. Soc.* **1987**, *109*, 3337.
(15) McCusker, J. K.; Christmas, C. A.; Hagen, P. M.; Chadha, R. K.; Harvey, D. F.; Hendrickson, D. N. *J. Am. Chem. Soc.* **1991**, *113*, 6114.
(16) Wieghardt, K.; Pohe, K.; Jibrie, I.; Hütther, G. *Angew. Chem., Int. Ed. Engl.* **1984**, *23*, 77.
(17) Hagen, K. S.; Armstorng, W. H. *J. Am. Chem. Soc.* **1989**, *111*, 774.
(18) Pope, M. T.; Müller, A. *Angew. Chem., Int. Ed. Engl.* **1991**, *30*, 34.
(19) Caneschi, A.; Gatteschi, D.; Sessoli, R.; Barra, A. L.; Brunel, L. C.; Guillot, M. *J. Am. Chem. Soc.* **1991**, *113*, 5873.
(20) Boyd, P. D. W.; Li, R.; Vincent, J. B.; Folting, K.; Chang, H. R.; Straib, W. E; Huffmann, J. C.; Christon, G.; Hendrickson, D. N. *J. Am. Chem. Soc.* **1988**, *110*, 8537.
(21) Micklitz, W.; Lippard, S. J. *J. Am. Chem. Soc.* **1989**, *111*, 6856.
(22) Müller, A.; Krickemeyer, E.; Penk, M.; Walberg, M. J.; Bögge, H. *Angew. Chem., Int. Ed. Engl.* **1987**, *26*, 1045.
(23) Müller, A.; Döring, J. *Angew. Chem., Int. Ed. Engl.* **1988**, *27*, 1721.
(24) Müller, A.; Penk, M.; Krickemeyer, E.; Bögge, H.; Walberg, M. J. *Angew. Chem., Int. Ed. Engl.* **1988**, *27*, 1719.
(25) Müller, A.; Penk, M.; Rohlfing, R.; Krickemeyer, E.; Döring, J. *Angew. Chem., Int. Ed. Engl.* **1990**, *29*, 926.
(26) Müller, A.; Döring, J.; Khan, M. I.; Wittueben, V. *Angew. Chem., Int. Ed. Engl.* **1991**, *30*, 210.
(27) Müller, A.; Rohlfing, R.; Bögge, H.; Döring, J.; Penk, M. *Angew. Chem., Int. Ed. Engl.* **1991**, *30*, 588.
(28) Müller, A.; Döring, J.; Penk, M. *Z. Anorg. Allg. Chem.* **1991**, *595*, 251.
(29) Müller, A.; Döring, J.; Bögge, H. *J. Chem. Soc., Chem. Commun.* **1991**, 273.
(30) Müller, A. *Nature* **1991**, *352*, 115.
(31) Müller, A.; Penk, M.; Döring, J. *Inorg. Chem.* **1991**, *30*, 4935.
(32) Gatteschi, D.; Pardi, L.; Barra, A. L.; Müller, A.; Döring, J. *Nature* **1991**, *354*, 463.

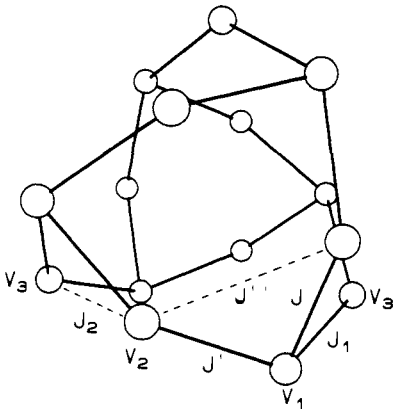

Figure 4. Outline of the vanadium ions of V_{15} and coupling constants.

Structure and Coupling Scheme for V_{14}

The structure[23] of V_{14} is shown in Figure 1. There are eight vanadium(IV) ions defining an octagon, plus two sets of three vanadium ions which connect diametrically opposed centers on the octagons, as shown in Figure 2. The overall symmetry of the clusters is D_{2d}. The exchange pathways connecting the equatorial V_3 and V_4 ions are identical by symmetry. All the equatorial vanadiums are bridged by two oxygen atoms, one of an oxo group and one of an arseniato group. The V_3–V_4 distances are 3.01 Å.

The exchange pathways involving the V_2–V_4 ions are determined by two oxo groups, with short V–V distances of 2.81 Å.

The exchange pathway V_2–V_1 is determined by two oxygen atoms belonging to two arseniato groups, with a V_1–V_2 distance of 3.06 Å. Another possible relevant exchange pathway is that connecting V_2 and V_3, with a V_2–V_3 distance of 3.60 Å and a single oxo bridge. All these exchange pathways are collected in Table I.

Structure and Coupling Scheme for V_{15}

The strucure[28] of V_{15} is shown in Figure 3. As far as the vanadium ions are concerned, they can be grouped in two distorted hexagons, sandwiching a central triangle, as shown in Figure 4. The V_1 atoms are connected to two V_2 atoms, with two different exchange pathways. The one corresponding to the shortest V–V distance, 2.87 Å, is formed by two oxo bridges, while the other, which corresponds to a V–V distance of 3.05 Å, is formed by a μ-oxo and a μ-arseniato group. V_1 is also connected to V_3 with a similar bridge, the V_1–V_3 distance being 3.02 Å.

V_2 is connected to another V_2 through a single μ-oxo bridge, corresponding to a V–V distance of 3.08 Å. A similar bridge also connects V_2 to V_3, with a distance of 3.73 Å. All the relevant exchange pathways are collected in Table I.

Extended Hückel Calculations

Well-characterized systems for which structural–magnetic correlations have been established for oxovanadium(IV) pairs are rather rare. As far as dinuclear complexes are concerned strong antiferromagnetic coupling (J = 354 cm^{-1}) was observed in a di-μ-hydroxo complex,[36,37] while in a μ-oxo bridged pair the complex was found to be diamagnetic at room temperature.[38] In addition, several μ-phosphate and μ-selenate bridges were reported to have antiferromagnetic couplings[33-35] ranging from 5 to ca. 60 cm^{-1}.

In order to interpret our complex compounds we decided to use extended Hückel calculations, which were satisfactorily used to rationalize the magnetic coupling in copper(II) pairs[40] in different geometries.

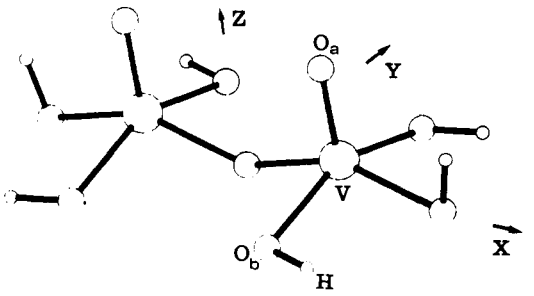

Figure 5. Model $VO(OH)_3O(OH)_3VO$ structure for extended Hückel calculations.

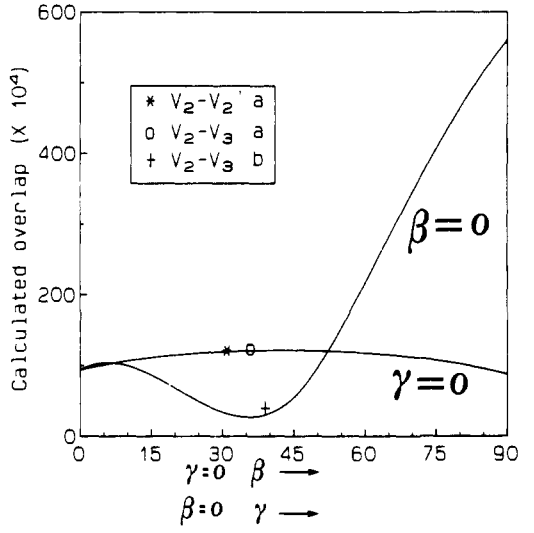

Figure 6. Overlap between the magnetic orbitals of the $VO(OH)_3$ and $VO(OH)_3O$ fragments. β and γ are defined in the text.

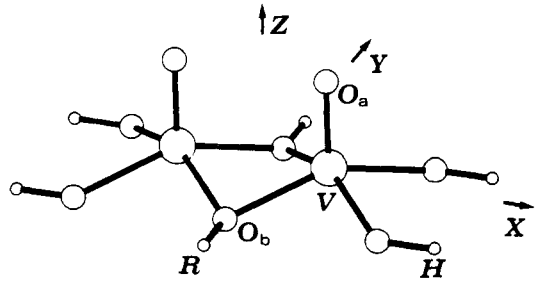

Figure 7. Model $VO(OH)_2(OR)_2(OH)_2VO$ structure for extended Hückel calculations.

For single μ-OR bridged pairs we used the geometry shown in Figure 5. The overlap between the magnetic orbitals was evaluated by using two asymmetric fragments, one $VO(OH)_3$ and one $VO(OH)_3(OR)$ group. The V–O distances in the bridge were kept constant at 195 pm, and one moiety was rotated relative to the other around the x, y, and z axes. The extent of the antiferromagnetic coupling is expected to depend on the squared overlap, S^2, between the two magnetic orbitals, which for oxovanadium(IV) complexes are essentially d_{xy} orbitals on the two metal centers. In Figure 6 we plot S as a function of the angle of rotation around y, β, for various values of the angle γ, defined

(33) Villeneuve, G.; Amoros, P.; Beltran, D.; Drillon, M. In *Organic and Inorganic Low Dimensional Crystalline Materials*; Delhaes, P., Drillon, M., Eds.; NATO ASI Series B168; Plenum Press: New York and London, 1987; p 417.
(34) Wroblewski, J. *Inorg. Chem.* **1988**, *27*, 946.
(35) Huan, G.; Johnson, J. W.; Jacobson, A. J.; Goshorn, D. P.; Merola, J. S. *Chem. Mater.* **1991**, *3*, 539.
(36) Ozarowski, A.; Reinen, D. *Inorg. Chem.* **1986**, *25*, 1704.
(37) Wieghardt, K.; Bossek, U.; Volckmar, K.; Swiridoff, W.; Weiss, J. *Inorg. Chem.* **1984**, *23*, 1387.
(38) Huan, G.; Johnson, J. W.; Jacobson, A. J.; Merola, J. S. *Chem. Mater.* **1990**, *2*, 719.
(39) Toftlund, H.; Larsen, S.; Murray, K. *Inorg. Chem.* **1991**, *30*, 3964.
(40) Hary, P. J.; Thibeault, J. C.; Hoffmann, R. *J. Am. Chem. Soc.* **1975**, *97*, 4884.

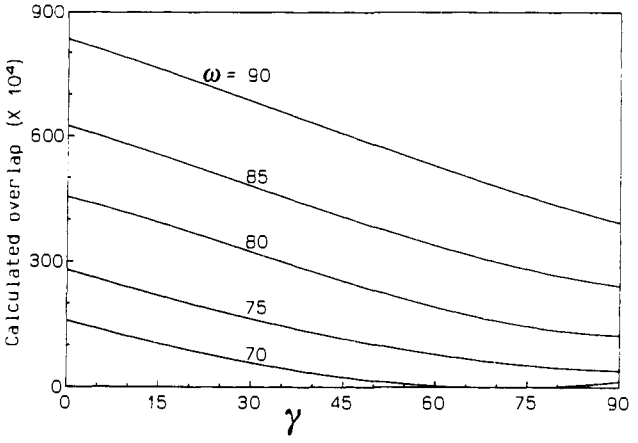

Figure 8. Overlap between the magnetic orbitals of $VO(OH)_2(OR)_2$-$(OH)_2VO$ of the $VO(OH)_2(OR)$ fragments. γ and ω are defined in the text.

as a rotation of one group relative to the other around z. The overlap is relatively small for $\beta = 0°$ and $\gamma = 0°$, due to the long distance between the two vanadium centers. An increase in β determines only a very small increase in S. In Figure 6 we plot also the variation of the overlap with γ, keeping β fixed at 0°. The overlap is initially practically constant, then decreases to reach a minimum at ca. 40°, and then increases dramatically. Beyond the mismatch of the lobes of the magnetic orbitals, the factor which determines the geometric variation of the overlap is the change in the V–V distance. In fact the V–V distance moves from 380 pm at $\gamma = 0°$ to 270 pm for $\gamma = 90°$. The points which are indicated in Figure 6 correspond to the bridges in the complexes under investigation with $\beta \approx 35°$, $\gamma \approx 30°$, i.e. to regions of relatively weak overlap. Therefore a relatively weak antiferromagnetic coupling can be anticipated for these complexes.

For di-μ-oxo bridges we used two identical moieties $VO(OH)_2(OR)$, with the geometry indicated in Figure 7. The angles that were taken into consideration are the O_b–V–O_b angles, ω, and the dihedral angle γ between the two planes of four basal oxygens. In Figure 8 is shown the variation of S as a function of γ, for various values of ω. The behavior is monotonic, with S decreasing on increasing γ and on decreasing ω. The experimental points correspond to complexes which have $\omega \approx 85°$ and $\gamma \approx 45°$. Since the overlap varies significantly in this range, consistent variations in the AF couplings of the systems can be expected. However, the extent of the coupling in these di-μ-oxo bridges is expected to be stronger than for single bridges.

Finally, as a general remark we can state that the shorter the V–O_b distance is the larger the coupling is. If the O^{2-} bridges are substituted by OH^- or OR^- groups the overlap decreases. Therefore it can be expected that the intensity of the antiferromagnetic coupling decreases in the order $O^{2-} > OH^- > OR^-$.

Magnetism and EPR Spectra of V_{14} and V_{15}

The temperature dependence of the χT product of V_{14} is shown in Figure 9. The room temperature value (2.48 emu mol^{-1} K, $\mu_{eff} = 4.45\ \mu_B$) is much smaller than expected for 14 uncoupled $S = {}^1/_2$ spins (5.25 emu mol^{-1} K), indicative of antiferromagnetic coupling. Initially χT decreases slightly on decreasing temperature, and it stabilizes at ca. 2.1 emu mol^{-1} K. Below ca. 150 K χT increases and reaches a maximum of ca. 2.3 emu mol^{-1} K at 15 K. Below 10 K χT decreases rapidly, reaching 1.78 emu mol^{-1} K at 1.9 K.

The temperature dependence of the χT product of V_{15} is shown in Figure 10. The roome temperature value (2.05 emu mol^{-1} K) is much smaller than expected for 15 uncoupled $S = {}^1/_2$ spins (5.625 emu mol^{-1} K). It decreases rapidly with decreasing temperature; below ca. 100 K the value stabilizes at about 1 emu mol^{-1} K, and below 20 K it starts to decrease again, reaching 0.5 emu mol^{-1} K at 1.8 K.

The EPR spectra of single crystals of V_{14} and V_{15} were recorded at low temperature, because the lines are too broad at room

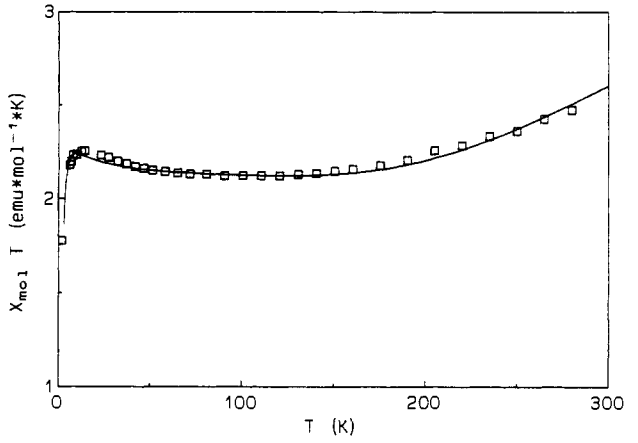

Figure 9. Experimental and calculated χT for V_{14}. For the parameters used see text.

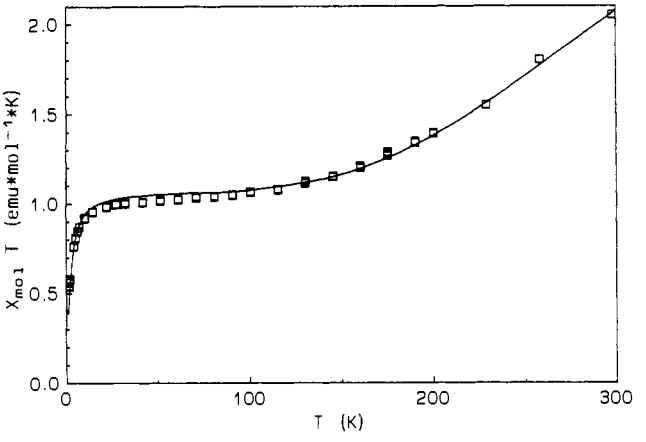

Figure 10. Experimental and calculated χT for V_{15}. For the parameters used see text.

temperature to observe any change in the crystal rotations. In the case of V_{14} we observed a completely isotropic **g** tensor and line width, as expected on the basis of the symmetry of the molecule. Sample dipolar second moment calculations[41] agree with an isotropic line width.

The EPR spectra of a single crystal of V_{15} were recorded at 25 K, i.e. in the temperature range where χT shows a plateau. The **g** tensor is anisotropic, with $g_c = 1.98$, $g_a = g_b = 1.95$. The peak-to-peak line width goes through a minimum in the 20–100 K temperature range.

The temperature dependence of the magnetic susceptibility (χT) of V_{15} is simpler to qualitatively interpret than that of V_{14}, and we will start form the former.

The initial decrease of χT with decreasing temperature, the plateau close to 1 emu mol^{-1} K, and the further decrease below 20 K are a clear indication that several exchange pathways, of different efficiency, operate in this cluster. The suggestion which emerges is that one or more exchange pathways are so strong that the two spins connected by them are in a singlet ground state at ca. 100 K. The residual value of χT suggests the presence of three substantially uncoupled spins. The further decrease at lower temperature must therefore be interpreted as the effect of other exchange pathways which become important below 20 K. This hypothesis is confirmed by the temperature dependence of the EPR spectra.

The anisotropy of the spectra can be reproduced assuming that the signal observed is the average of the signals of the three V_3 ions. In fact these have their V=O directions (practically) perpendicular to the crystal trigonal axis and make angles of 120° between themselves. It is well-known that oxovanadium(IV) ions

(41) Bencini, A.; Gatteschi, D. *EPR of Exchange Coupled Systems*; Springer Verlag: Berlin, 1990.

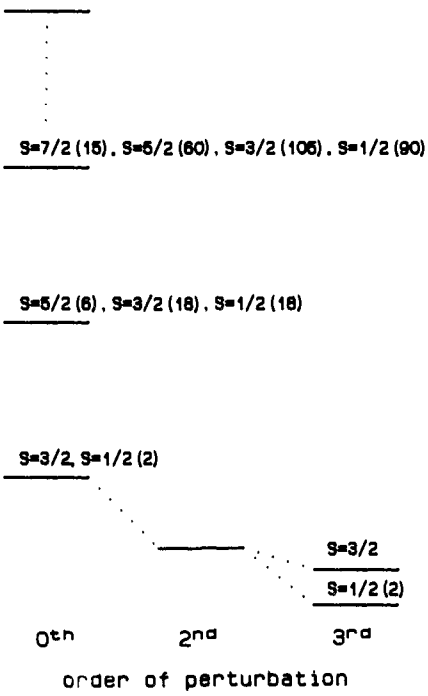

Figure 11. Lowest lying energy levels of V_{15} calculated with a perturbation approach.

are characterized by $g_\parallel \simeq 1.93$, $g_\perp \simeq 1.98$, with $g_\parallel$ along the V=O direction. Therefore the three V_3 ions will all have $g_\perp$ along the crystal c axis, while in the plane perpendicular to c they will average to $g_{av} = [(g_\parallel^2 + g_\perp^2)/2]^{1/2} = 1.95$. In this way we must expect that in the crystal $g_c = g_\perp$, $g_a = g_b = g_{av}$, in excellent agreement with experiment. Inspection of the coordinates of the other vanadium ions shows that no other set of atoms of V_{15} is oriented in a similar way. Therefore the EPR spectra unambiguously identify the V_3 ions as responsible for the residual magnetism of the cluster below 100 K. Therefore it must be assumed that at least one of the pathways connecting the V_1 and V_2 atoms is very effective in transmitting strong antiferromagnetic coupling. We assume that the bis μ-oxo bridges are the ones responsible of the strong antiferromagnetic coupling between V_1 and V_2. In favor of this hypothesis is the short metal–metal distance associated to these bridges, which gives the possibility of direct V–V overlap. Further it is well-known that μ-oxo bridges are more effective than μ-hydroxo or μ-alkoxo bridges in transmitting antiferromagnetic exchange interactions between several transition metal elements. Finally this result is supported by the extended Hückel calculations of the previous section.

Magnetism and Energy Levels of V_{15}

Perturbation Approach. On the basis of the above considerations we try to interpret the magnetic properties of V_{15} assuming that J is much larger than all the other coupling constants. Whether this is a reasonable assumption or not must be verified a posteriori by the ability of the model that can be developed to reproduce the experimental χT versus T plot. On the basis of this hypothesis a perturbation approach will be possible.

If J is much larger than all the other coupling constants, then the high-temperature behavior of the magnetic susceptibility will only be due to the splitting of the spin levels introduced by this strong interaction, all the others being neglected. In this case we obtain that the lowest energy level is the one with all the pairs V_1 and V_2 in their ground $S = 0$ state and the V_3 ions independent. Thus this energy level for the cluster is eight times degenerate, corresponding to two doublets and a quartet. The excited states can be formed by exciting one or more V_1–V_2 pair in the triplet state, still considering the V_3 spins as uncoupled. In Figure 11 a scheme of the lowest energy levels is given, with the indication of the degeneration of each of them, according to the indications given above.

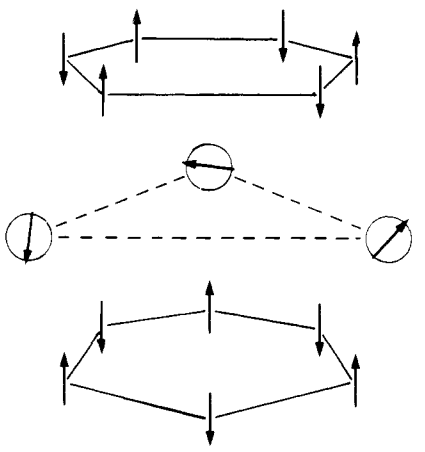

Figure 12. Preferred spin orientations on the magnetic planes of V_{15}.

Table II. Dimensions of the Matrices for the Total Spin Values of V_{14} and V_{15}

V_{14}		V_{15}	
S	dimensions	S	dimensions
7	1	15/2	1
6	13	13/2	14
5	77	11/2	90
4	273	9/2	350
3	637	7/2	910
2	1001	5/2	1638
1	1001	3/2	2002
0	429	1/2	1430

The low-temperature behavior of the susceptibility ($kT \ll J$) can be described considering only the 8-fold degenerate ground level and taking into account the weaker interactions in a perturbative way. In this approach we obtain a splitting of the ground state only at the third order of perturbation. This results from the fact that two V_3 ions are coupled to each other through either an exchange pathway V_3–V_2–V_2–V_3 or V_3–V_1–V_1–V_3. The energy splitting between the two $S = {}^1/_2$ and ${}^3/_2$ states belonging to the ground configuration is $\Delta E = {}^3/_4(J_1 - J_2)^2(J' - J'')/J^2$, where the coupling constants are defined in Table I. $\Delta E > 0$ means that the $S = {}^3/_2$ state is the ground state. As can be seen from the above formula, it is not possible to determine the individual J_1, J_2, J', and J'' coupling constants, but only the combinations which are present in the expression for ΔE. Thus we will make the approximation $J_1 - J_2 \approx J' - J''$, an approximation which is also justified by the geometry of the cluster. The fit of the magnetic susceptibility, reported in Figure 10, gives $J = 556$ cm^{-1}, $J_1 - J_2 = J' - J'' = -104$ cm^{-1}.

Complete Calculation. In order to test the validity of the perturbation approach we performed a complete calculation of the energy levels of V_{15} within the spin hamiltonian formalism. In order to do this we used an irreducible tensor operator, ITO, approach recently developed by two of us[42] which allows a fast and efficient calculation of the energy levels of HNSC. The dimensions of the matrices involved in the calculations are given in Table II. We only used the set of parameters deduced by the perturbative approach for the sake of simplicity. In particular we used $J = 525$ cm^{-1}, $J' = 20$ cm^{-1}, $J'' = 124$ cm^{-1}, $J_1 = 20$ cm^{-1}, $J_2 = 124$ cm^{-1}. We did not try to fit the individual constants because the perturbative approach showed that they are not independent from each other. The calculated susceptibility is almost superimposable to that obtained within the simplified approach.

The full matrix provides the energies of all the spin levels as shown in Figure 13. It is apparent that the groud $S = {}^1/_2$ and ${}^3/_2$ states are very close to each other. On increasing energies the separations of the levels decreases, so that at high energies almost a continuum is formed. This is indeed one of the feature

(42) Gatteschi, D.; Pardi, L. *Gazz. Chim. Ital.* In press.

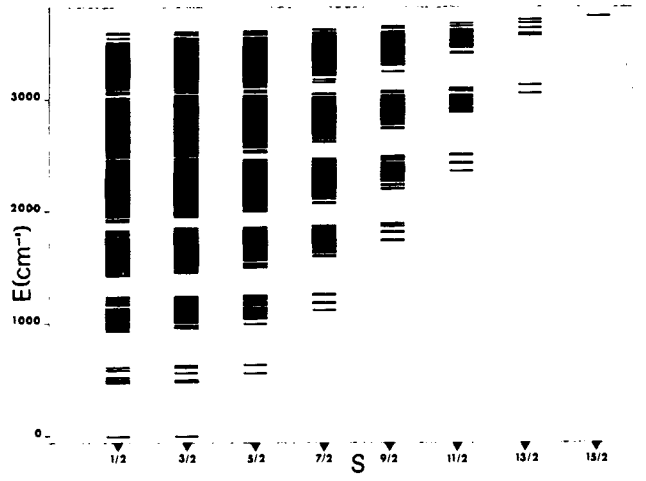

Figure 13. Calculated total spin energy levels for V_{15}.

of HNSC, which makes them similar to infinite assemblies of spins.

The picture which emerges from the magnetic structure of V_{15} is extremely interesting. In fact there are three layers with different magnetic properties: the two hexagons are completely coupled, and they can mimic antiferromagnetic layers, while the spins in the triangle are frustrated, as pictorially indicated in Figure 12. It must be stressed that the three spins in the triangle are actually coupled to the other spins, but it is the result of the topology of the magnetic interactions which leaves them only weakly coupled. So V_{15} can be considered as a simple model of a magnetic multilayer structure with two antiferromagnetic layers sandwiching a triangular layer.

Although the results of the analysis of the magnetic properties of V_{15} can be considered as encouraging, the basic assumptions which were used must be critically tested before concluding on the validity of the approach. Therefore it is of fundamental importance that the properties of V_{14} are interpreted similarly.

Magnetism and Energy Levels of V_{14}

In V_{14}, as in V_{15}, the high-temperature magnetic moment clearly indicates that some exchange interactions are more effective than others, because χT stabilizes at ca. 1.9 emu mol^{-1} K. If we assume that the di-μ-oxo bridges correspond to very strong antiferromagnetic coupling, as for V_{15}, we may assume that at relatively high temperature the V_2–V_4 pairs are in the ground $S = 0$ state, thus leaving the four V_3 and the two V_1 ions substantially uncoupled, in agreement with the value of the plateau of χT which corresponds to six unpaired electrons.

At lower temperature also the V_3 and V_1 ions will start to feel each other through the J_1, J_2, and J_3 coupling constants. If we assume that they are all antiferromagnetic, the ground state of the cluster will be determined by the relative strength of J_2 compared to J_3. For both $J_2 > J_3$ and $J_2 < J_3$ the spins of the V_3 ions will tend to be parallel between themselves and so will the spins of the V_1 ions. If $J_2 > J_3$ the spins of the V_3 ions will be antiparallel to those of the V_1 ions. Therefore the expected ground state of the cluster is $S = 1$ in this case. If on the other hand $J_3 > J_2$ the spins of the V_3 and V_1 ions will be parallel to each other, and a ground state $S = 3$ is expected. The experimental value of χT at low temperature better agrees with a ground $S = 1$ state, indicating that $J_2 > J_3$. A comparison with the values obtained for V_{15}, where J_2 and J_3 are comparable, suggests that small changes in the geometry of the bridges can induce changes in the coupling constants.

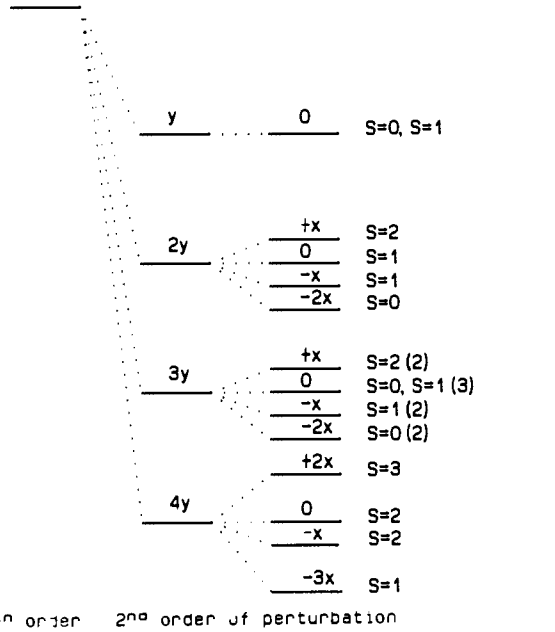

Figure 14. Low-lying energy levels of V_{14} calculated with a perturbation approach: $x = J_1(J_2 - J_3)/2J$, $y = -(J_2 - J_3)^2/2J$.

Also for V_{14} it is possible to attempt a perturbation treatment if J is assumed to be much larger than all the other coupling constants. Therefore the lowest levels of the clusters can be described with the four V_2–V_4 pairs in the ground $S = 0$ state to give a total spin $S = 0$. The remaining six spins give a total of 64 states as shown in Figure 14. The excited states can be formed by exciting one or more V_2–V_4 pairs in the triplet state to yield the states of multiplicity indicated in Figure 14. The fit of the magnetic susceptibility, reported in Figure 9, gives $J = 507$ cm^{-1}, $J_2 - J_3 = 69$ cm^{-1}, and $J_1 = 19$ cm^{-1}.

Also in this case we tested the validity of the perturbative approach by performing complete calculations. We used the following values of the constants: $J = 486$ cm^{-1}, $J_1 = 19$ cm^{-1}, $J_2 = 124$ cm^{-1}, $J_3 = 55$ cm^{-1}. Also in this case the agreement between the two models is very good.

Conclusions

The investigation of the magnetic properties of V_{14} and V_{15} has shown how using variable-temperature magnetic susceptibility and EPR spectra can allow a reasonably detailed understanding of the preferred spin arrangement in high nuclearity spin clusters. The fast computers now available, in conjunction with irreducible tensor methods, which take the maximum advantage of the total spin symmetry, provide valuable tools in order to express the energies of the spin levels. However, qualitative considerations on the relative ability of different exchange pathways to provide efficient couplings between different metal ions are mandatory in order to reduce the number of independent parameters.

Finally, one of the reasons why the investigation of high nuclearity spin clusters appears to be desirable is that they should mimic the properties of bulk magnets. Indeed we have found in nuce such a behavior in V_{15}, which behaves as a magnetic multilayer, and also in V_{14}, where many different spin orientations in different zones of the molecule are observed.

Acknowledgment. The financial support of MURST, CNR, and Progetto Finalizzato Materiali Speciali per Tecnologie Avanzate is gratefully acknowledged.